THE JOURNAL OF PHYSICAL CHEMISTRY B

Article

pubs.acs.org/JPCB

Hydrothermally Mixed Hydroxyapatite–Multiwall Carbon Nanotubes Composite Coatings on Biomedical Alloys by Electrophoretic Deposition

C. B. Ustundag,[†] O. Avciata,[†,‡] F. Kaya,[‡] and C. Kaya*[,‡]

[†]Vocational School, Yildiz Technical University, Maslak, Istanbul, Turkey

[‡]Metallurgical and Materials Engineering Department, Yildiz Technical University, Davutpasa, Istanbul, Turkey

ABSTRACT: Hydroxyapatite (HA) coatings have been used to improve biological and mechanical fixation of metallic prosthesis. Because of extraordinary features of carbon nanotubes (CNTs), they have a lot of facilities, such as extremely strong nanoreinforcement materials for composites. HA powders were synthesized and mixed with multiwalled carbon nanotubes (MWCNTs) by a hydrothermal process. Calcium acetate ($Ca(CH_3COO)_2$) and phosphoric acid (H_3PO_4) were used as starting materials for synthesizing nano-HA powders. HA–MWCNTs were treated together hydrothermally at 200 °C for 2 h to synthesize nano-HA powders mixed homogeneously with MWCNTs. Cathodic deposits were obtained on Ti-based alloys using suspensions containing nano-HA and MWCNTs dispersed in *n*-butanol solvent. It was shown that MWCNTs interacted with HA powders during hydrothermal processing, and therefore, they can easily be dispersed within aqueous-based suspensions. It was also shown that hydrothermal surface modification of MWCNTs with functional groups was achievable, which was a significant step toward eliminating nonwetting surface behavior of MWCNTs, resulting in obtaining homogeneous dispersion of them in liquids.

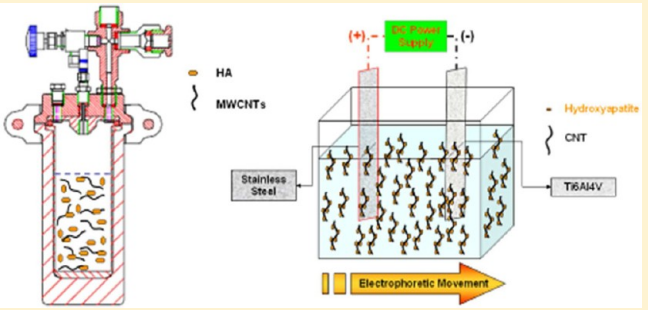

INTRODUCTION

In order to improve osteoconductive properties, metallic implants, such as Ti alloys, are coated with bioactive layers including hydroxyapatite [$Ca_{10}(PO_4)_6(OH)_2$] (HA) or bioactive glass for encouraging the in-growth of natural bone into the prosthetic device using some coating technologies, such as plasma spraying,[1] dip coating,[2] biomimetic coating,[3] sol–gel coating,[4] and electrophoretic deposition.[5]

Mineralogical and chemical properties of HA ceramics are similar to bone, and they do not exhibit any toxic effects with surrounded tissue. These properties are required for bone generation and substitute materials for damaged bones. However, mechanical properties of HA ceramics are not sufficient for load-bearing applications. Therefore, ceramic materials, such as ZrO_2,[6] Al_2O_3,[7] SiC,[8] and CNT[9] have been used to fabricate HA-based composites with improved mechanical properties. CNTs can be used as additives to reinforce composite materials, such as polymer, metal, and ceramic matrix composites,[10−14] due to their excellent physical and mechanical properties. They have been used as extremely strong nanoreinforcements for composites that possess extraordinarily high strength with low weight and moderate electrostatic discharge properties.[15] However, obtaining homogeneous nanocomposites with carbon nanotubes remains a technical challenge.[16] Commercially available CNTs are generally too long to be dispersed in solution and have no well-defined functional groups to modify.[17] Therefore, CNTs have poor dispersion properties in a liquid because of hydrophobic surfaces, while surface modification of the CNTs provides efficient dispersion and stability of the suspension.

Electrophoretic deposition (EPD) has advantages of low equipment cost, short formation time, simplicity in instrumentation, and capability of coating complex-shaped implants[18−21] (see Figure 1). EPD is a colloidal process that provides easy control of thickness and quality of coating through simple adjustment of the deposition time, applied potential, and powder morphology.[22] It is capable of forming complex shapes and patterns[18,19] as the deposition of colloidal particles is carried out under a DC voltage.[23,24] In the present work, a composite coating of HA– carbon nanotubes (CNTs) on Ti alloys was prepared using hydrothermally mixed suspensions containing surface-functionalized CNTs by EPD.

HA powder and CNT surface modification was obtained by a hydrothermal technique. Generally, CNT surface functionalization is provided by acidic treatments, such as a $HNO_3 + H_2SO_4$ mixture (3:1), to give them a negative surface charge due to presence of OH, COO, and COOH groups.[25−28] Here, we have focused on CNT surface functionalization without acidic

Special Issue: Electrophoretic Deposition

Received: May 24, 2012
Revised: July 10, 2012

   dx.doi.org/10.1021/jp305057p | *J. Phys. Chem. B* XXXX, XXX, XXX–XXX

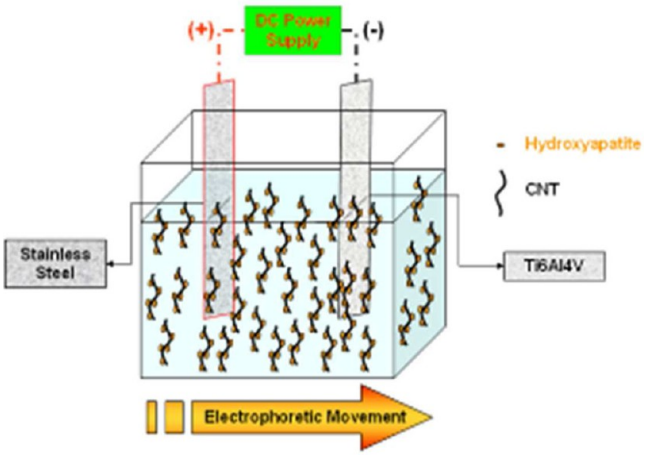

Figure 1. Schematic illustration of the EPD cell and HA−CNTs particle groups.

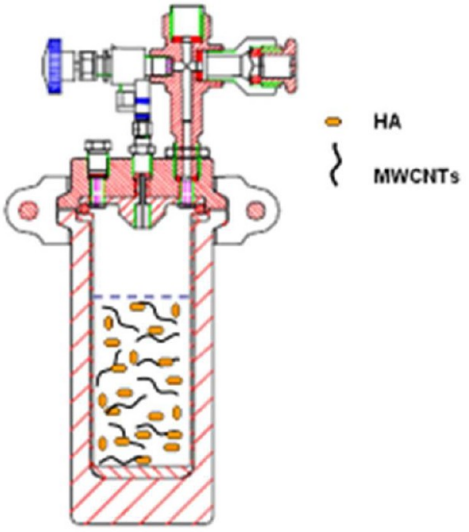

Figure 2. Hydrothermal reactor (adopted from Berghof GmbH).

treatment to eliminate possible surface damage on CNTs. Hydrothermal surface modification has some advantages; it is a greener and economic technology and has a shortened process time and steps (it should also be noted that acidic treatment of CNTs diminishes the physical properties, such as mechanical strength, and causes geometric failure, while hydrothermal synthesis (HS) eliminates all these disadvantages).

Therefore, in the present work, successful results on the processing of CNT-reinforced HA layers on Ti-based alloys with a high degree of homogeneity using the EPD technique are presented. Surface functionalization of CNTs was achieved during hydrothermal processing so that they could be dispersed or mixed with other particles in a liquid environment.

EXPERIMENTAL METHODS

A nanosize hydroxyapatite and multiwalled carbon nanotubes (MWCNTs) mixture was prepared by the hydrothermal method. HA was synthesized using calcium acetate ($Ca(CH_3COO)_2$) and phosphoric acid (H_3PO_4) as starting materials, with a molar ratio of 10:3, and an ammonia solution as the agent for pH adjustment. Calcium acetate was dispersed in distilled water, and ammonia solution was added to calcium acetate solution to adjust the solution to pH $\geq$ 10. H_3PO_4 was slowly added dropwise to the calcium acetate solution and was vigorously stirred, and the pH of the mixture was balanced to $\geq$10. MWCNTs (10−30 nm in diameter, up to 30 μm in length, and with 40−300 m^2/g surface area (Shenzen Nanotechnologies Co Ltd., China)) were used. The prepared hydroxyapatite solution was mixed with 1 wt % MWCNTs and ultrasonicated for 5 min. The solution was transferred into a Teflon liner. For the hydrothermal process, 200 mL of a HA−CNTs suspension was put in a Teflon (PTFE)-lined autoclave (see Figure 2) and into the hydrothermal unit (Berghof BR300 High Pressure Reactor, Germany). The experimental run was carried out in vessels made of SS 316 L, at 200 °C for 2 h. The run product was repeatedly washed with distilled water and dried at 100 °C in an oven overnight.

Hydrothermally processed HA + MWCNTs powders were dispersed and ultrasonically mixed in *n*-buthanol for 3 h. Suspensions containing 1 wt % MWCNTs of the total powders were prepared for coating experiments. A constant suspension solid loading of 2 wt % was used for all experiments. EPD experiments were conducted under DC voltage conditions (30 V) for different deposition times. Stainless steel electrodes with a separation distance of 20 mm were used for all coating experiments.

Hydroxyapatite powders were characterized using scanning electron microscopy (SEM), energy-dispersive X-ray spectroscopy [FEGSEM (JEOL JSM 7000F), EDX (Oxford/Inca)], and transmission electron microscopy (TEM, HF-2000, Hitachi). X-ray diffraction (XRD) was performed using the Shimadzu XRD-6000 to observe the phases formed. The infrared spectra of the hydroxyapatite nanoparticles were obtained using the Perkin− Elmer system 2000 FTIR-ATR. The specific surface areas of the synthesized powders were determined by the Brunauer−Emmett−Teller (BET) method using a surface area analyzer (Quantachrome-NOVA 2200e). The particle sizes of the HA powders were observed by a laser diffraction particle size analyzer (LDPA, Better Size Inc. BTH 9300).

RESULTS AND DISCUSSION

Figures 3 and 4 show the SEM and TEM micrographs of HA and the HA−CNTs mixture. As shown in Figure 3a, the synthesized HA powders are on the nanoscale, and there is a tendency to form agglomerates due to the high surface area of nano-HA particles. However, the hydrothermally synthesized HA−CNTs powder mixture does not contain any large agglomerates, as shown in Figure 3b, which proves the presence of well-mixed HA−CNTs particles.

Further TEM observations reveal that hydrothermally synthesized HA powders actually have a rod-like shape with a length of 60−70 nm and a width of 10−15 nm, as shown in Figure 4a. A homogeneous mixture of HA−CNTs particles during HS is achieved, as shown in Figure 4b. This particle morphology is considered to be beneficial to obtain a porous HA layer (after sintering), which increases the mechanical bonding between the coating layer and natural bone. It can be concluded from Figures 3 and 4 that by using these powder mixtures, stable homogeneous dispersions of HA and MWCNTs are prepared using the hydrothermal method. As shown in the SEM micrograph in Figure 3b and the TEM micrograph in Figure 4b, adequate mixing of the HA powder and CNTs was achieved, and no preferential agglomerates of

dx.doi.org/10.1021/jp305057p | J. Phys. Chem. B XXXX, XXX, XXX−XXX

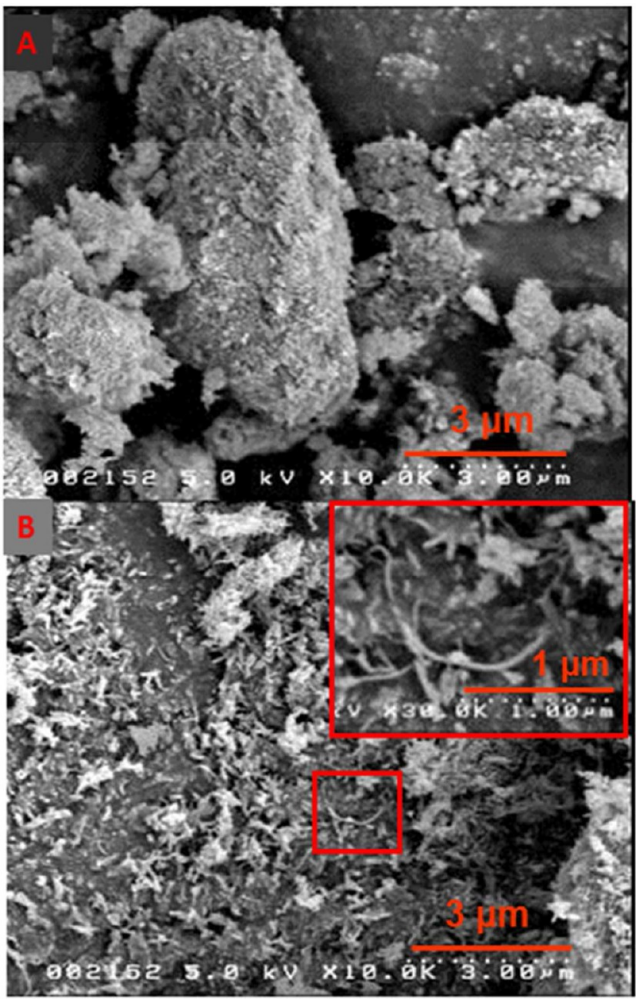

Figure 3. SEM micrograph of hydrothermally processed HA (A) and the HA−CNTs mixture (B) after drying.

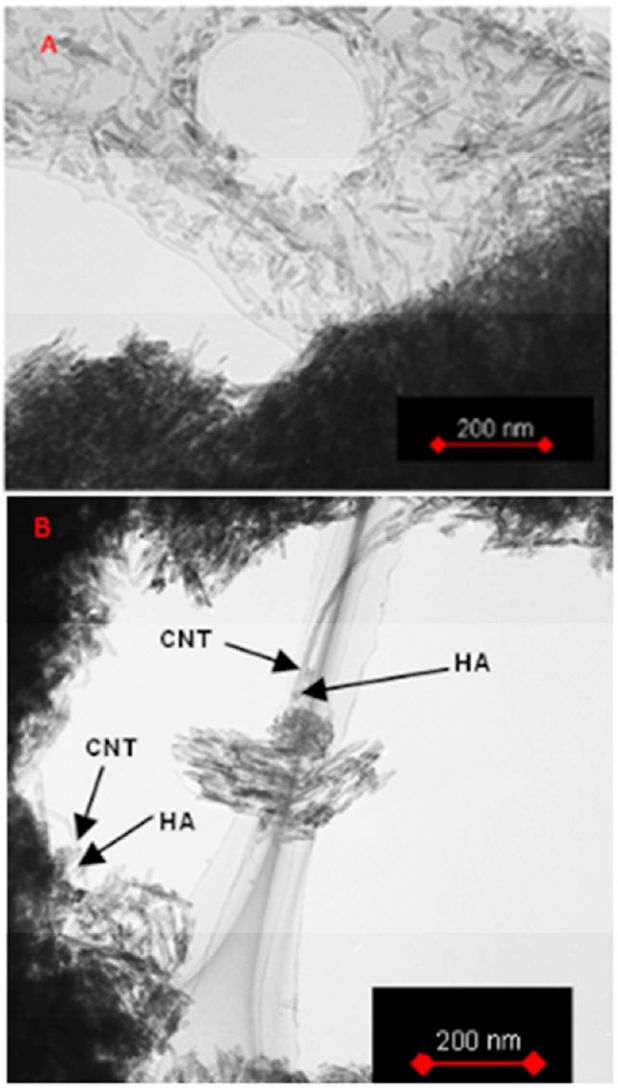

Figure 4. TEM micrograph of hydrothermally processed HA (A) and the HA−CNTs mixture (B).

HA powders or CNTs were observed, confirming that the suspensions were well-dispersed and stable.

Furthermore, FT-IR spectra of HA−CNTs powders showed some functional groups, such as hydroxyl and carboxylic groups, as shown in Figure 5. These groups provide surface functionalization of CNTs during the hydrothermal process. During the hydrothermal process, an increase in pH helped the precipitation and formation of the HA ($Ca_5(PO_4)_3(OH)$) phase. Ammonia solution was used for pH balancing, and the overall reaction is given.

$$5Ca(CH_3COO)_2 + 3H_3PO_4 + 10NH_3 + H_2O \rightarrow Ca_5(PO_4)_3(OH) \downarrow + 10NH_4CH_3COO_{(aq)} + OH^-_{(aq)} \quad (1)$$

$NH_4CH_3COO_{(aq)}$ (ammonium acetate) and $OH^-_{(aq)}$ (hydroxyl) groups in reaction 1 supply surface functionalization during the hydrothermal process. The absorption bands at 1565 (−COOH) and 1420 cm^{-1} (−COO) prove the presence of carboxylic groups, which is proposed to come from the precipitation process. The carboxylic groups' peaks decrease with CNTs adding to HA due to surface functionalization of CNTs during the hydrothermal process (see Figure 5). FT-IR spectra shown in Figure 5 proved that CNT surface modification was achieved by the hydrothermal process, resulting in obtaining the HA−CNT powder mixture, which can easily be dispersed in liquids.

The surface charge of HA and CNTs is adjusted to be opposite so that they can attract each other and act as a single-composite particle during the hydrothermal process under the application of high pressure and applied heat. BET (see Table 1) and laser diffraction particle size analyses verify these phenomena. Normally, CNTs do not show good wetting properties, but some carboxylic acid and other oxygen-containing groups on the CNT surface increase the wettability. These functional groups electrostatically stabilize the CNTs in water or other polar liquids by means of negative surface charge, which considerably increases the stability of suspensions. Due to interaction of HA−CNTs, HA particles move on the CNT surface because of negative surface charge (see Figure 3b). Consequently, a nanocomposite structure comes into existence with the increase of mechanical properties and decrease of crack and peeling of the coating layer after the sintering process.

XRD patterns of HA and HA−MWCNTs powders are shown in Figure 6. The XRD result of HA powder as a

dx.doi.org/10.1021/jp305057p | J. Phys. Chem. B XXXX, XXX, XXX−XXX

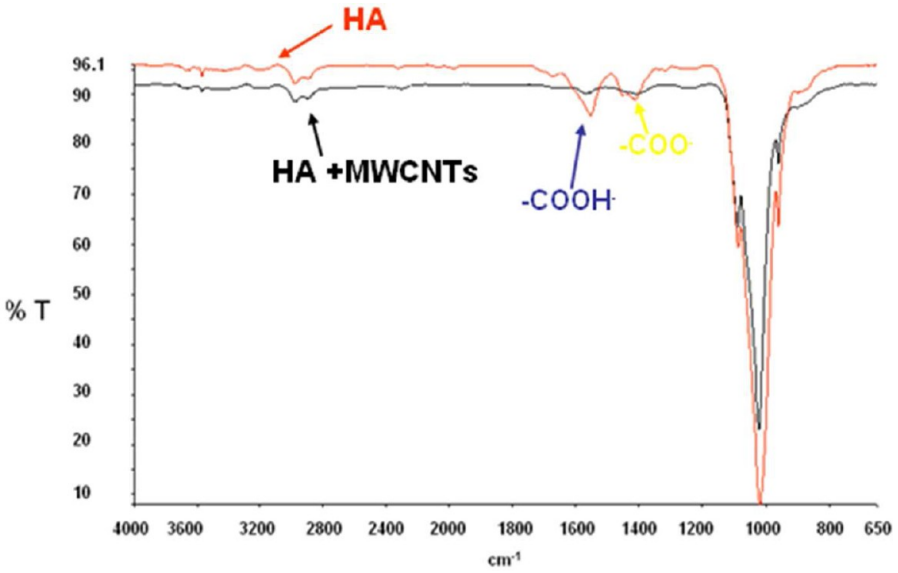

Figure 5. The FT-IR spectra of HA and HA−MWCTs powders.

Table 1. BET Surface Area, TEM Observation, and Laser Diffraction Particle Analyzer (LDPA) Results of As-Precipitated HA and Hydrothermally Processed HA−CNT Powders

sample	surface area (m^2/g) BET	$length_{ave}$ (nm) TEM	$diameter_{ave}$ (nm) TEM	d_{ave} (μm) LDPA
HA	58	46	9	11.45
HA + MWCNTs	37	67	10	14.87

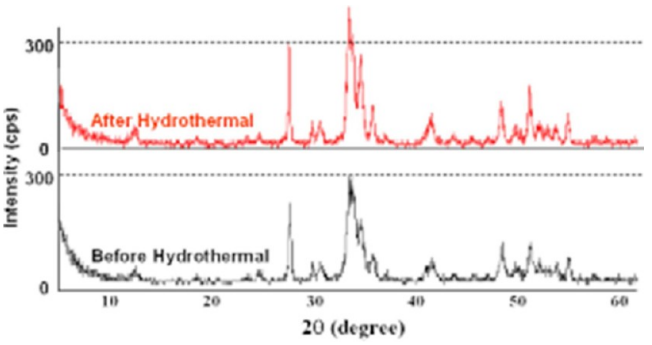

Figure 6. XRD analysis of HA (as-precipitated) and HA + MWCNTs (hydrothermally treated).

precipitated material is shown in Figure 6, indicating that the synthesized powders have no anhydrous calcium phosphate phase and all of the peaks correspond to the formation of stoichiometric HA (JSPDS Card No. 09-432).

As is very well known, crystallinity and crystal size increase with hydrothermal treatment. The wide peaks shown in Figure 6 could be the low crystallinity and indicate the formation of small-size HA powders. TEM diffraction pattern observations proved this condition, as shown in Figure 7. Figure 7a shows the TEM diffraction pattern of as-precipitated HA, which is brighter than hydrothermally treated HA (Figure 7b). This indicates that the hydrothermally processed HA−CNTs have higher crystallinity. XRD studies show that after the hydrothermal treatment, there is an increase in the crystallinity and

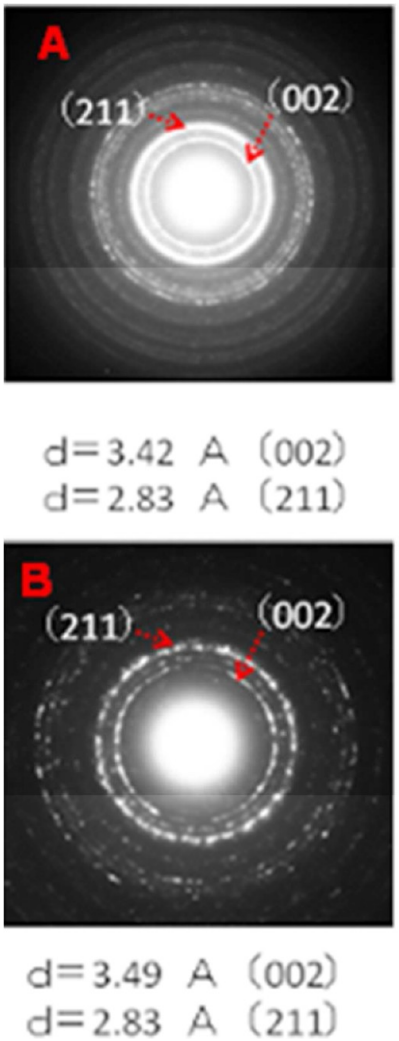

Figure 7. TEM diffraction patterns of as-precipitated HA (A) and hydrothermally treated HA + MWCNTs (B).

crystal size. Table 1 shows the effect of hydrothermal treatment on the crystal size of nano-HA.

dx.doi.org/10.1021/jp305057p | J. Phys. Chem. B XXXX, XXX, XXX−XXX

Table 1 shows the information about the particle size of the synthesized HA and HA−CNTs powder mixture. The particle surface areas of the as-precipitated HA and hydrothermally treated HA−CNTs are found to be 58 and 37 m^2/g, respectively, as shown in Table 1. The TEM observations show that there is a slight increase in the size of the HA−CNTs powder mixture (from 46 to 67 nm for the length and from 9 to 10 nm for the diameter) compared to that for HA due to hydrothermal treatment. LDPA results show that the increase in the size is due to coverage of CNTs by HA particles. It is also seen from Table 1 that there is an increase in particle size (or partly flocculated group HA−CNT) and a decrease in surface area because of the interaction between HA and CNTs with the hydrothermal process. HA nanoparticles tend to attach to the surface of CNTs during the hydrothermal process. Stable mixtures containing HA and HA−CNT particles were obtained as shown in Figure 8 for coating experiments.

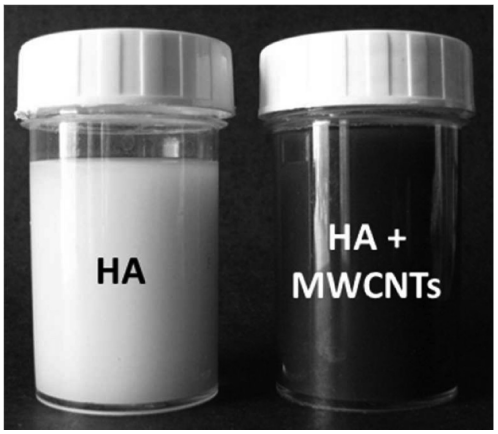

Figure 8. Stable colloidal suspensions of HA and a HA−MWCNTs mixture.

The SEM micrographs shown in Figures 3 and 4 are in a good agreement with the picture shown in Figure 8, both proving the presence of kinetically stable suspensions as CNTs repel each other after surface functionalization in the hydrothermal process and, therefore, that they are well-dispersed and make a good combination with HA particles in suspension.

Figure 9 shows the EPD thickness dependence of the coating layers on the coating time. Results were obtained using suspensions with a constant solid loading of 2 wt % (in the HA + CNTs suspension, the weight ratio between HA and CNTs was kept at 99/1), applied voltage of 30 V DC, and an electrode separation distance of 20 mm. Deposition times were between 20 and 180 s. In the EPD process, the amount of accumulation can be explained by Henry's equation.[29]

$$w = f\frac{2}{3}C\varepsilon_0\varepsilon_r\zeta\left(\frac{1}{\eta}\right)\left(\frac{V_{app}}{L}\right)t \quad (2)$$

where f is the Hamaker factor, w is the deposited weight on the substrate, C is the particle concentration in suspension, ε_0 is the permittivity of a vacuum, ε_r is the relative permittivity of the solvent, ζ is the zeta potential, η is the viscosity of the solvent, V_{app} is the applied electric voltage, L is the distance between the anode and cathode, and t is the deposition time.

According to Anné et al., the applied electric field, V_{app}, decreases with increased coating thickness. This phenomenon

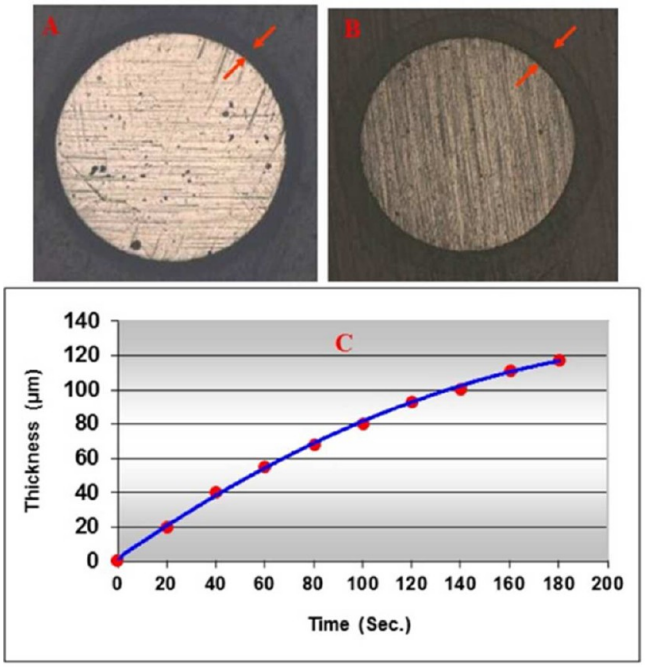

Figure 9. The images of Ti6Al4V coatings as a function of time [(A) 90 s; (B) 180 s] and a graph of the coating layer thickness (μm) of Ti6Al4V alloys versus time during the EPD process (C).

was expressed by the following equation in their study.[30] The applied voltage drop over the deposit is given by

$$V_{real} = V_{app}\left(1 - \frac{d_{dep}}{d_{dep} + (L - d_{dep})r_{suspension}/r_{deposit}}\right) \quad (3)$$

with d_{dep} being the thickness of the deposit, L as the distance between the electrodes, and V_{app} being the applied voltage, $r_{deposit}$ as the deposit resistivity, and $r_{supension}$ as the suspension resistivity.

The deposit weight is related to the coating thickness in the EPD process.[22,31] According to the results, the coating layer thickness is increased by the duration of progress, but the slope of the curve is decreased by increasing deposition time, as shown in Figure 9. The deposition thickness−time study showed that saturation of the coatings occurred at around 180 s, with ∼120 μm for the HA−MWCNTs suspension. However, for the HA suspension, the coating experiments under similar conditions, coating thickness ∼110 μm for 180 s, were observed. The reason for this difference is thought to arise from the coating layer contained in MWCNTs. It is well-known that MWCNTs are conductive materials. Therefore, MWCNTs affect the conductivity of composite materials.[32,33] Obtained results show that the HA−MWCNTs coating layers are thicker than the HA coating layers. Because of these differences, the coating layers consisting of HA−MWCNTs and MWCNTs affect the conductivity of the coating layers. This case can be associated with eq 3. In addition, as shown in Table 1, during the hydrothermal process, HA interacts with MWCNTs, and flocculation occurrs. This flocculation might be supplied by porous and thicker coating layers than the HA coating layers. Besides, CNT dispersion in a matrix affects the mechanical and electrical properties. If CNTs have good dispersion ability, composite materials perform desired properties. The hydrothermal process could provide a suitable combination between

dx.doi.org/10.1021/jp305057p | J. Phys. Chem. B XXXX, XXX, XXX−XXX

HA and CNTs and not generate a defect on the CNTs. Therefore, expected properties from coatings, such as mechanical, electrical, and thermal, with CNTs can be obtained by the hydrothermal process.

CONCLUSION

Nanosized HA is produced (and mixed with CNTs) by hydrothermal synthesis at 200 °C for 2 h, which provides an effective and novel surface modification/functionalization for CNTs as well as a homogeneous mixture, without phase segregation. Addition of CNTs to HA decreases the surface area due to the HA particles' move to the CNT surface during the hydrothermal process. The method described here allows the surface modification of CNTs and adequate mixing of HA−CNTs. EPD is successfully utilized to create HA + CNTs coating layers on medical-grade Ti alloys. The results showed that the time of deposition was an important factor for the coating process. Besides, the deposition of particles on the coating electrode surface causes a decrease in the suspension concentration and electric field, resulting in a decrease in the coating layer. EPD provides a HA−MWCNTs coating layer thickness of 120 μm for a deposition time of 180 s.

AUTHOR INFORMATION

Corresponding Author

*E-mail: cengizk@yildiz.edu.tr.

Notes

The authors declare no competing financial interest.

ACKNOWLEDGMENTS

This work was funded by TUBITAK (The Scientific and Technological Research Council of Turkey) under Contract Number 108T651. The Yildiz Technical University Scientific Research Fund is also acknowledged for support under Contract No. 2010-07-02-DOP01. Special thanks to Prof. Dr. Koji Ioku and Assoc. Prof. Dr. Masanobu Kamitakahara of Tohoku University for SEM and TEM facilities.

REFERENCES

(1) Filaggi, M. J.; Coombs, N. A.; Pilliar, R. M. *J. Biomed. Mater. Res.* **1991**, *25*, 1211−1229.
(2) Boulton, L. M.; Gregson, P. J.; Tuke, M.; Baldwin, T. *Mater. Lett.* **1991**, *12*, 1−6.
(3) Wei, M.; Uchida, M.; Kim, H.; Kokubo, T.; Nakamura, T. *Biomaterials* **2002**, *23*, 167−172.
(4) Milev, A. S.; Kannangara, G. K.; Ben-Nissan, B. *Mater. Lett.* **2003**, *57*, 1960−1965.
(5) Zhitomirsky, I.; Gal-Or, L. *J. Mater. Sci.: Mater. Med.* **1997**, *8*, 213−219.
(6) Ioku, K.; Yoshimura, M.; Somiya, S. *Biomaterials* **1990**, *11*, 57−61.
(7) Li, J.; Fartash, B.; Hermansson, L. *Interceram* **1990**, *36*, 20−23.
(8) Noma, T.; Shoji, N.; Wada, S.; Suzuki, T. *J. Ceram. Soc. Jpn.* **1992**, *100*, 1175−1178.
(9) Chen, Y.; Gan, C. H.; Zhang, T. H.; Yu, G.; Bai, P.; Kaplan, A. *Appl. Phys. Lett.* **2005**, *86*, 251905/1−251905/3.
(10) Jia, Z. J.; Wang, Z. Y.; Xu, C. L.; Liang, J.; Wei, B. Q.; Wu, D. H.; Zhu, S. W. *Mater. Sci. Eng., A* **1999**, *271*, 395−400.
(11) Kuzumaki, T.; Miyazawa, K.; Ichinose, H.; Ito, K. *J. Mater. Res.* **1998**, *13*, 2445−2449.
(12) Dong, S. R.; Tu, J. P.; Zhang, X. B. *Mater. Sci. Eng., A* **2001**, *313*, 83−87.
(13) Flahaut, E.; Peigney, A.; Laurent, C. H.; Marlière, Ch; Chastel, F.; Rousset, A. *Acta Mater.* **2000**, *48*, 3803−3812.
(14) Xu, C. L.; Wei, B. Q.; Ma, R. Z.; Liang, J.; Ma, X. K.; Wu, D. H. *Carbon* **1999**, *37*, 855−858.
(15) Kin-Tak, L.; David, H. *Carbon* **2002**, *40*, 1605−1606.
(16) Wagner, H. D.; Lourie, O.; Feldman, Y.; Tenne, R. *Appl. Phys. Lett.* **1998**, *72*, 188−190.
(17) Sano, M.; Kamino, A.; Okamura, J.; Shinkai, S. *Science* **2001**, *293*, 1299−1301.
(18) Sarkar, P.; Nicholson, P. S. *J. Am. Ceram. Soc.* **1996**, *79*, 1987−2002.
(19) Boccaccini, A. R.; Zhitomirsky, I. *Curr. Opin. Solid State Mater. Sci.* **2002**, *6*, 251−260.
(20) Van der Biest, O.; Vandeperre, L. J. *Annu. Rev. Mater. Sci.* **1999**, *29*, 327−352.
(21) Heavens, S. N. *Electrophoretic deposition as a processing route for ceramics. Advanced Ceramic Processing and Technology*; Noyes Publications: Park Ridge, NJ, 1990; pp 255−283.
(22) Besra, L.; Liu, M. *Prog. Mater. Sci.* **2007**, *52*, 1−61.
(23) Singh, I.; Kaya, C.; Shaffer, M. S. P.; Thomas, B. C.; Boccaccini, A. R. *J. Mater. Sci.* **2006**, *41*, 8144−8151.
(24) Kaya, C. *J. Eur. Ceram. Soc.* **2003**, *23*, 1655−1660.
(25) Kaya, C. *Ceram. Int.* **2008**, *34*, 1843−1847.
(26) Kaya, C.; Singh, I.; Boccaccini, A. R. *Adv. Eng. Mater.* **2008**, *10*, 1−8.
(27) Lin, C.; Han, H.; Zhang, F. *J. Mater. Sci.: Mater. Med.* **2008**, *19*, 2569−2574.
(28) Kaya, C.; Kaya, F.; Cho, J.; Roether, J. A.; Boccaccini, A. R. *Key Eng. Mater* **2009**, *412*, 93−97.
(29) Hunter, R. J. *Foundations of Colloid Science*; Oxford University Press: Oxford, U.K., 1989, 265−270.
(30) Anné, G.; Neirinck, B.; Vanmeensel, K.; Van der Biest, O.; Vleugels, J. *J. Am. Ceram. Soc.* **2006**, *89*, 823−828.
(31) Ciou, S. J.; Fung, K. Z.; Chiang, K. W. *J. Power Sources* **2008**, *175* (1), 338−344.
(32) Zaman, A. C.; Ustundag, C. B.; Celik, A.; Kara, A.; Kaya, F.; Kaya, C. *J. Eur. Ceram. Soc.* **2010**, *16* (30), 3351−3356.
(33) Zaman, A. C.; Ustundag, C. B.; Kaya, F.; Kaya, C. *Ceram. Int.* **2012**, *2* (38), 55−59.